IIETA International Information and Engineering Technology Association
Advancing the World of Information and Engineering

Mathematical Modelling of Engineering Problems
Vol. 11, No. 11, November, 2024, pp. 2912-2918
Journal homepage: http://iieta.org/journals/mmep

Simulation and Analysis of n-Type Electron Blocking Layers in GaN-Based Light-Emitting Diodes

Wassila Kazi Tani*, Siham Khedim, Sofiane Amara

Materials and Renewable Energy Research Unit, University of Abou-Bekr Bekaid, Tlemcen 13000, Algeria

Corresponding Author Email: w_kazi_t2002@yahoo.fr

https://doi.org/10.18280/mmep.111104

Received: 23 August 2024
Revised: 13 October 2024
Accepted: 20 October 2024
Available online: 29 November 2024

Keywords:
light-emitting diode, aluminum gallium nitride, Indium gallium nitride, efficiency droop

ABSTRACT

This study presents a gallium nitride (GaN) based light-emitting diode (LED) structure with nine period of 2nm/3nm thick n-type $In_{0.05}Ga_{0.95}N/Al_{0.15}Ga_{0.85}N$ electron blocking layer (EBL) inserted between the active region and n-GaN cladding layer is numerically designed, and examined using physical device simulator SILVACO. The proposed structure is compared with the p-$Al_xGa_{(1-x)}N$ EBL cladding layer. The obtained results indicate that, the introduction of InGaN layers in n- type EBL seems to be an efficient solution to decrease electron overflow and enhance hole injection efficiency by keeping a low indium concentration. The droop is improved from 25.07% to 34.57% when we switch from p-type $Al_{0.15}Ga_{0.85}N$ to n-type $In_{0.05}Ga_{0.95}N/Al_{0.15}Ga_{0.85}N$.

1. INTRODUCTION

Light-emitting diodes (LEDs) have many advantages, efficient, high durability, low production cost, and can be integrated into technology architectures for digital display applications. For several years, III-N semiconductors have dominated the light-emitting diode industry, due to their opto-electronic properties. In general, p-type p-$Al_xGa_{(1-x)}N$ electron blocking layer (EBL) was inserted in LED device to suppress electron leakage. Several designs of EBL devices have been published. For example, effect of electron blocking layer on the efficiency of AlGaN mid-ultraviolet light emitting diodes by Pandey et al. [1], Al-composition-graded AlGaN/GaN superlattice EBL (GSL-EBL) by Park et al. [2], quantum efficiency enhancement by employing specially designed AlGaN electron blocking layer by Usman et al. [3], thickness-graded quantum barriers and composition-graded electron blocking layer for efficient green light-emitting diodes by Usman et al. [4], high performance of a Non-Polar AlGaN-Based DUV-LED with a Quaternary Superlattice Electron Blocking Layer by Dai et al. [5]. Electroluminescence study of InGaN/GaN QW based p-i-n and inverted p-i-n junction based short-wavelength LED device using laser MBE technique par Yadav et al. [6]. However, the p-type doping of EBL has some limitations. Excellent p-type doping is necessary for the EBL to achieve low layer resistance [7]. In addition to, the ineffective Mg-doping leads to very low concentrations of free holes in AlGaN [8, 9]. Second, the conduction band barrier of the EBL blocking electrons on the active region side also leads to simultaneous formation of a valence band barrier blocking holes on the p-type region side, thereby impeding hole injection [10, 11], resulting in lower recombination rate and poor internal quantum efficiency (EQE), called droop. However, on the other hand, electron concentrations in the range of ~10^{18}-$10^{19}$$cm^{-3}$ can be readily achieved in n-type AlGaN using silicon as a dopant [12, 13]. Nevertheless, despite their achievements, GaN/InGaN LEDs continue to have drawbacks that prevent them from reaching their maximum efficiency potential. Controlling the passage of charge carriers, especially electrons, inside the device structure is one of the main technological difficulties. By lowering the probability of radiative recombination in the active region, this phenomenon known as electron overflow can lower LED efficiency. This emphasises the necessity of creating efficient ways to stop these electrons, which is why electron blocking layers are so crucial.

By reducing electron overflow out of the active region, electron blocking layers (EBL) have historically enhanced performance in GaN/InGaN LEDs. Early EBL designs made extensive use of materials like AlGaN. By improving the radiative recombination of electrons with holes, these EBLs were successful in raising the device's overall efficiency. However, because of their valence band misalignment with the InGaN active material, AlGaN layers frequently offer disadvantages, such as putting obstacles to hole injection. The internal quantum efficiency (IQE) of the device may be compromised as a result of inadequate hole injection into the active region. By adjusting material thicknesses and compositions, several research have attempted to counteract this effect; however, these changes frequently involve trade-offs between decreasing electron overflow and increasing hole injection efficiency [4]. As a result, current methods that use p-type AlGaN based EBLs have a number of drawbacks. First of all, they do not optimise hole injection at the same time, even though they successfully restrict electron overflow. Second, these layers produce significant valence band discontinuities that raise the device's series resistance, thereby increasing the voltage drop and causing losses in electrical

efficiency.

Designing a new EBL architecture that addresses these problems without sacrificing LED performance is essential in light of these difficulties. An n-type $In_{0.05}Ga_{0.95}N/Al_{0.15}Ga_{0.85}N$ EBL is proposed in this study with the goal of minimising electron overflow while preserving high hole injection. Additionally, we propose incorporating a nine-period EBL inserted between the active region and the n-GaN layer, designed to operate at ~460 nm, in order to enhance electron blocking capability without affecting hole injection. We simulate the effect of the n-type $In_{0.05}Ga_{0.95}N/Al_{0.15}Ga_{0.85}N$ insertion layer on band diagrams, current density, IQE, power spectral density, and radiative recombination rate. We found that n-type $In_{0.05}Ga_{0.95}N/Al_{0.15}Ga_{0.85}N$. EBL insertion layer can effectively reduce electron overflow and improve hole injection efficiency in the device active region. This results in improved current density, IQE, and radiative recombination rate. The voltage drop is improved from 25.07% to 34.57% when switching from p-type $Al_{0.15}Ga_{0.85}N$ to n-type $In_{0.05}Ga_{0.95}N/Al_{0.15}Ga_{0.85}N$.

2. MODELING APPROACH

To reduce the time required with fabrication cost to analyse and optimise the proposed LEDs device, we use the industrial simulation SILVACO [14]. The electrical property of the LEDs was performed by solving the Poisson's equation and the continuity equation. The transport model of electrons and holes used in our simulation is drift-diffusion, this model was selected for its balance between accuracy and simplicity in carrier transport. The material dependent physical models that have been implemented with the models statement are: K.P multiband k.p, FERMI Fermi-Dirac carrier statistics, these models are essential for describing the interactions between bands and the distribution of carriers, incomplete ionization of impurities in Fermi-Dirac statistic this model reflects the actual carrier concentration in heavily doped regions, POLARIZATION the simulator will apply a piezoelectric polarization calculated using the strain value assigned by the strain parameter, this piezoelectric polarization is incorporated to account for the internal electric fields, which are prominent in GaN/InGaN materials. The models for quantum wells are: CHUANG gain-radiative recombination models, SPONTANEOUS included the radiative recombination rates derived from the Chuang model into the drift diffusion and LORENTZ Lorentzian line broadening. Also, the three bulk recombination mechanisms enabled on a model statement are SRH, AUGER and OPTR. The models of radiative recombination and non-radiative mechanisms effectively model the quantum wells and the losses in light efficiency.

The Shockley-Read-Hall recombination rate [15, 16] is modeled as follows in Eq. (1):

$$R_{SRH} = \frac{pn - n_i^2}{\tau_p \left[n + n_i exp\left({}^{\Delta E}/_{kT_l}\right)\right] + \tau_n \left[p + n_i exp\left({}^{-\Delta E}/_{kT_l}\right)\right]} \quad (1)$$

where, n and p are electron and hole concentrations, n_i is carrier intrinsic concentration, ΔE is the difference between the trap energy level and intrinsic Fermi level, T_l is the lattice temperature, τ_n and τ_p are the electron and hole lifetimes. Values given in literature for τ_n and τ_p usually vary from 30nm [17, 18] at 500nm [19] and are function of epitaxial quality material [20-22].

Auger recombination is commonly modeled using the expression Eq. (2) [10]:

$$R_{AUGER} = C_n(pn^2 - nn_i^2) + C_p(np^2 - n_i^2) \quad (2)$$

where, C_n and C_p are respectively auger coefficients for processes *eeh* and *ehh* (the excess momentum and energy can either be transferred to another electron or to another hole). The values of C_n and C_p vary between 10^{-34} and 10^{-29} [20, 21].

The radiative recombination is expressed by Eq. (3):

$$R_{OPT} = A(np - n_i^2) \quad (3)$$

A is bimolecular recombination coefficient. For *III-V* direct gap semiconductors, the A factor has values between $10^{-11}cm^3.s^{-1}$ and $10^{-9}cm^3.s^{-1}$.

The bandgap of $Al_xGa_{(1-x)}N$ and $In_xGa_{(1-x)}N$ as a function of the aluminum and indium composition x, is described by Eqs. (4) and (5) [23]:

$$E_g\left(Al_xGa_{(1-x)}N\right) = E_g(AlN)x + E_g(GaN)(1-x) - 1.3x(1-x) \quad (4)$$

$$E_g\left(In_xGa_{(1-x)}N\right) = E_g(InN)x + E_g(GaN)(1-x) - 3.8x(1-x) \quad (5)$$

Dirichlet boundary conditions were employed for the metal contacts in this study's SILVACO simulations, whereas Neumann boundary conditions were used to model fluxes. Charge transport equations could be resolved quickly due to the iterative solver that was employed for the simulations. To guarantee exact convergence, the tolerance threshold was chosen at 10^{-6}. To capture gradients in crucial areas like the p-n junction and the electron blocking layer, a thin and irregular mesh was used. Carrier mobility was taken to be isotropic, and several simplifications were made, such as excluding temperature effects and crystal flaws. To make the model less complicated, several simplification assumptions were also introduced. For example, carrier mobility was believed to be isotropic and surface effects and crystal defects were not expressly taken into account. Additionally, in this initial set of simulations, heat effects were disregarded.

3. DEVICE STRUCTURES AND PARAMETERS

To validate our device models and parameters we have considered the conventional p-$Al_xGa_{(1-x)}N$ electron blocking layer with~460nm wavelength emission (denoted as LED A). The structure and geometrical parameters of the light-emitting diode (mentioned LED) are based on those mentioned in literature. For example, the LED simulated by Ahmad et al. [24] or by Lu et al. [25]. This light-emitting diode consists (from top to bottom) of a3µm thick n-GaN layer (Si-doping=$1\times10^{19}cm^{-3}$), an active region comprises of five intrinsic layers of 3nm thick $In_{0.22}Ga_{0.85}N$ quantum well (QB) sandwiched between six intrinsic layer of a 15nm thick GaN quantum barrier (QB), a 45nm thich p-$Al_{0.15}Ga_{0.85}N$ EBL layer (Mg- doping=$1\times10^{19}cm^{-3}$), an a2µm thick p-GaN layer (Mg-doping=$5\times10^{18}cm^{-3}$). The composition of 22% indium in the $In_{0.22}Ga_{0.78}N$ quantum well was chosen based on previous studies which demonstrate that this concentration allows tuning the LED emission in the blue region (~460nm). Several studies, notably those of Verzellesi et al. [26], used similar

compositions for efficient blue LEDs, indicating that indium contents between 20% and 25% optimize optoelectronic performance while managing the mechanical stresses induced by the mesh difference between InGaN and GaN. In addition, this composition ensures a good compromise between the extension of the bandgap and the management of stress effects in quantum wells. Higher indium contents would increase stresses in the structure, potentially leading to defects that degrade efficiency. The schematic diagram of LED A is represented in Figure 1 (A). To decrease electron overflow without affecting hole injection into the active region, we proposed and studied numerically design in this section effect of $n-$type electron blocking layer (denoted as LED B). Nine period of 2nm/3nm thick n-type $In_{0.05}Ga_{0.95}N/Al_{0.15}Ga_{0.85}N$ electron blocking layer (Mg- doping=$1\times10^{19}cm^{-3}$) inserted between the active region and $n-GaN$ cladding layer of the device. The crucial material parameters used for $In_{0.05}Ga_{0.95}N$ and $Al_{0.15}Ga_{0.85}N$ electron blocking layer have been listed in Table 1. The performance characteristics of these device (LED B) is compared with device LED A. The rationale for the use of these particular materials is that, although AlGaN improves hole transport, InGaN can offer superior electron confinement because of its smaller energy bandgap. The 5% indium concentration of InGaN aids in preserving equilibrium between efficient electronic confinement and a decrease in defects associated with mechanical strain in the lattice. In order to provide a sufficiently enough band offset to block electrons without unduly penalising hole transport, AlGaN with 15% aluminium is used. The InGaN layers typically have thicknesses of 2nm for each superlattice period, while the AlGaN layers typically have thicknesses of 3nm. These numbers are chosen to create a potential barrier that efficiently prevents electrons from passing through while allowing holes to do so. This concept aims to get over the drawbacks of conventional p-type AlGaN EBLs. Because of the large band offset between AlGaN and the active region in InGaN, typical p-type AlGaN layers efficiently block electrons but have poor hole injection efficiency. We thus obtain better electron blocking by switching to an n-type EBL with the active region and $n-GaN$ cladding layer of the device. The schematic diagram of LED B is represented in Figure 1 (B). Figure 1 (C) and Figure 1 (D) show the equilibrium energy band diagram for LED A and LED B. It is remarked that there is a reduced barrier to holes injection in the active region for the two LEDs.

Table 1. Material parameters values used in SILVACO

Material Parameters	$In_{0.05}Ga_{0.95}N$	$Al_{0.15}Ga_{0.85}N$
χ_e	2.8	3
ε_r	8.9	9.3
E_g	3.08	9.2
m_n	$0.2m_0$	$0.2m_0$
m_p	$1.5m_0$	$1.8m_0$
C_{opt}	1.1×10^{-8}	1.1×10^{-8}
Aug_n	1×10^{-34}	1×10^{-34}
Aug_p	1×10^{-34}	1×10^{-34}
τ_n	1×10^{-9}	1×10^{-9}
τ_p	1×10^{-9}	1×10^{-9}

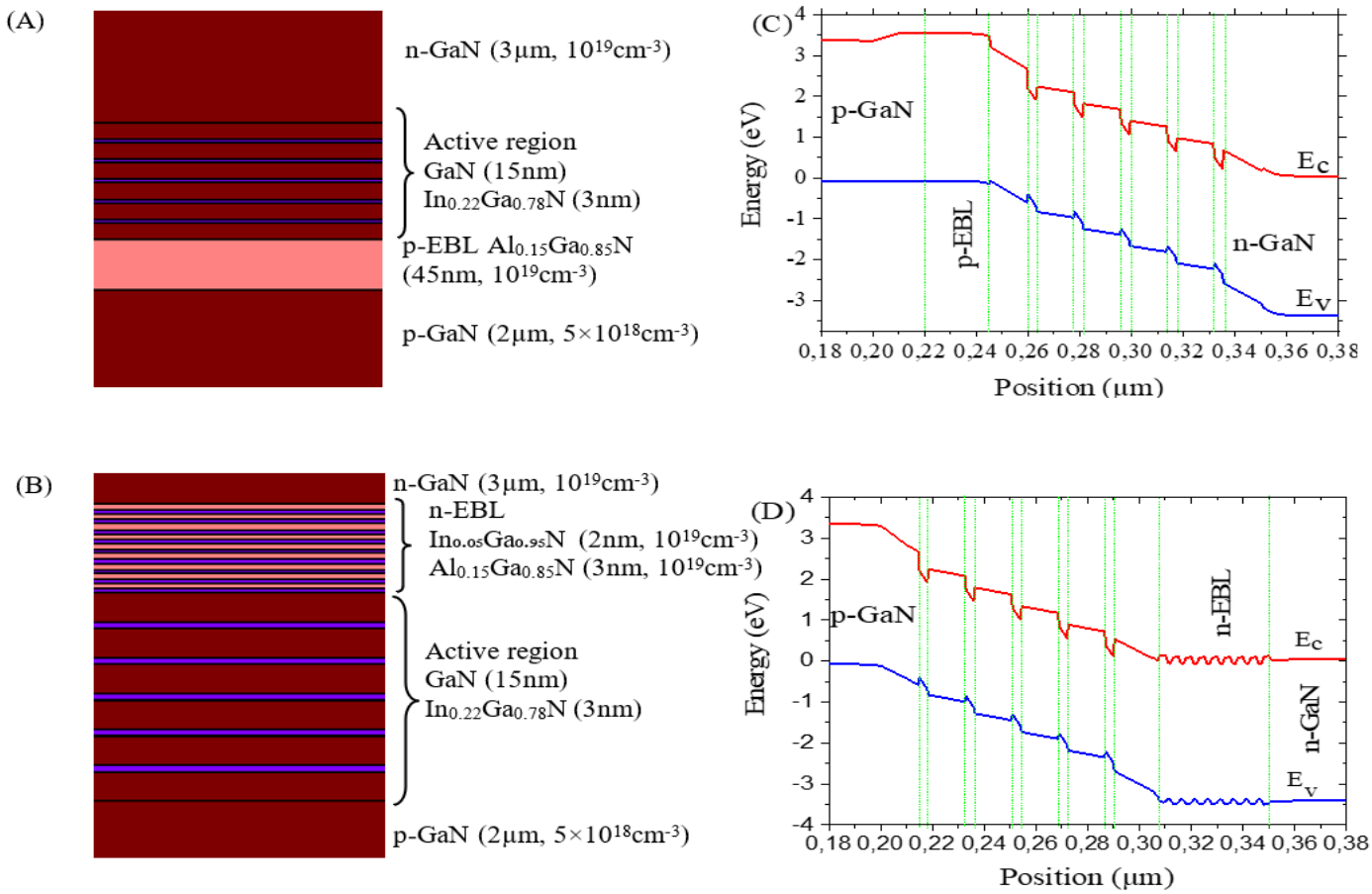

Figure 1. (A) Schematic illustration of conventional light-emitting diode (LED A); (B) A n-type $In_{0.05}Ga_{0.95}N/Al_{0.15}Ga_{0.85}N$ electron blocking layer (EBL); (C) Equilibrium energy band for the conventional device and (D) an n-type $In_{0.05}Ga_{0.95}N/Al_{0.15}Ga_{0.85}N$.EBL

4. RESULTS AND DISCUSSION

For a comparative study, we performed a numerical simulation on two LED structures. Structure A (LED A) uses a conventional p-type $Al_{0.15}Ga_{0.85}N$ EBL, whereas structure B (LED B) incorporates an n-type EBL with nine periods n-type $In_{0.05}Ga_{0.95}N/Al_{0.15}Ga_{0.85}N$. EBL before the active region. In order to increase the electron barrier height in LED devices, the application of an electron blocking layer (EBL) composed of $Al_xGa_{1-x}N$ has been investigated [27, 28]. However, because aluminium and gallium atoms differ in size, adding more aluminium increases lattice strain even while it improves electron confinement and decreases electron leakage from the active region. By introducing crystal defects and raising non-radiative recombination rates, especially through Shockley-Read-Hall (SRH) processes, this strain can lower the overall efficiency of the device. Additionally, research suggests that these pressures may weaken the layer's structural integrity, endangering the device's electrical and optical functionality. Also, some research has looked into EBL-free structures [29], which optimise the composition of the quantum well to lower the internal electric field. However, this might not offer the same degree of carrier confinement as a well-designed EBL.

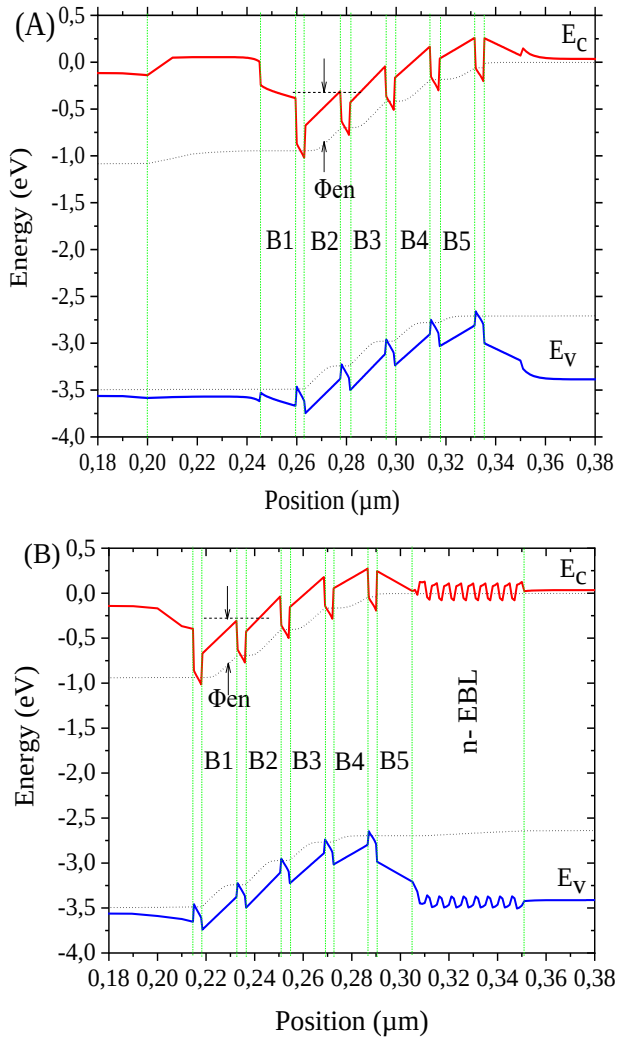

Notes: The black dotted lines indicate the quasi-Fermi levels. The green dotted lines indicate the positions of five quantum wells and EBLs

Figure 2. Energy band diagrams of Led A and Led B at an injection current at 3.5V bias

Figure 2 shows the calculated energy band diagrams of the two LEDs at 3.5V bias. In this Figure 2, Φ_{en} represents the potentiel barrier height in barrier B_1, B_2, B_3, B_4 and B_5 respectively. It is worth noting that the significant conduction and valence band bending at the barrier interfaces is more pronounced in the quantum wells when the voltage is non-zero. In blue LEDs, this strong energy band bending increases with the concentration of indium. This phenomenon leads to a distinct separation of the wave functions, known as the stark effect. The inherent polarities of III-N materials lead charge carriers to separate under the presence of a strong internal electric field, which results in the Stark effect seen in the quantum wells of InGaN-based LEDs. In contrast to the traditional LED A, the band structure of LED B is drastically changed by the insertion of n-type $In_{0.05}Ga_{0.95}N/Al_{0.15}Ga_{0.85}N$ layers before to the active region. This change lessens the Stark effect by improving the lowering of the electric field and band bending in the quantum wells. Due to its periodic multi-layer structure, LED B's improved electron confinement further inhibits electron overflow and enhances radiative recombination, both of which are critical for light efficiency.

The values for each potential barrier height for electrons in LED A and LED B at a 3.5V bias are extracted from the energy band diagrams and listed in Table 2. In both LEDs, the values of ϕ_{en} progressively decrease with each barrier, effectively blocking electron overflow. The obtained results show that the values of ϕ_{e2}, ϕ_{e3}, ϕ_{e4} and ϕ_{e5} are higher in LED B.

Table 2. Potential barrier height for electrons in LED A and LED B at 3.5V bias

	ϕ_{e2}(meV)	ϕ_{e3}(meV)	ϕ_{e4}(meV)	ϕ_{e5}(meV)
LED A	388	368	353	334
LED B	406	390	380	355

The probability of electron overflow from the active region is decreased by these values, which indicate improved electron-blocking capabilities. This promotes more effective radiative recombination and decreases non-radiative recombination by maintaining a better balance between electrons and holes in the quantum wells. The polarisation effects in the $In_{0.05}Ga_{0.95}N/Al_{0.15}Ga_{0.85}N$ EBL area can be used to explain this performance gain in LED B. In fact, band bending and carrier confinement are directly influenced by spontaneous and piezoelectric polarisation, which is especially important in III-nitride materials. These factors cause carrier separation (Stark effect) in the quantum wells, which lowers radiative recombination efficiency. Polarisation, particularly in AlGaN, produces an electric field in the EBL, however, which better restricts electrons in the active region. By decreasing electron overflow, this phenomenon, which is seen in the LED B structure, improves radiative recombination and raises the LED's overall efficiency. It is also noted that the maximum potential barrier height for electrons in this LED is 406 meV. Consequently, the electron-blocking capability in the active region of LED B is improved compared to LED A.

Figure 3 displays the distribution of the hole and electron current densities for both LEDs at 3.5V and 5V bias. The overall shape of both distributions is the same. The recombination mechanisms within the quantum wells seem to use up almost all of the hole current. In contrast, a substantial amount of the electron current escapes via the p-GaN and is not used up by the recombination process in the quantum well region. One of the main things limiting the effectiveness of

traditional LEDs is this electron leakage. Due to significant non-radiative recombination and inadequate electron confinement, this leakage is especially noticeable in the case of LED A. In contrast, LED B has a larger current density, which suggests better electron confinement. In LED B, the hole current densities are much greater at 325.88A/cm², 316.92A/cm², 299.81A/cm², and 246.05A/cm² (jp lower than jn), but the electron current densities in the first four quantum wells at 3.5V bias are 10.66A/cm², 17.99A/cm², 34.25A/cm², and 88.67A/cm², respectively. The electron and hole current densities in the fifth quantum well, on the other hand, almost perfectly match j_holes=j_electrons=134.96A/cm² pour la LED A et j_holes=j_electrons=163.79A/cm² pour la LED B. The 21.38% increase in current density in your proposed structure demonstrates a more efficient injection of carriers into the active region. The electron current densities in LED B keep getting better at 5V bias. For instance, the electron and hole current densities in the fourth quantum well are exactly equal (j_holes=j_electrons=15.69mA/cm²). Since the electron current density in the fifth quantum well is somewhat larger than the hole current density (j_electrons=19.62mA/cm² and j_holes=12.80mA/cm²), radiative recombination is improved due to better control over electron overflow.

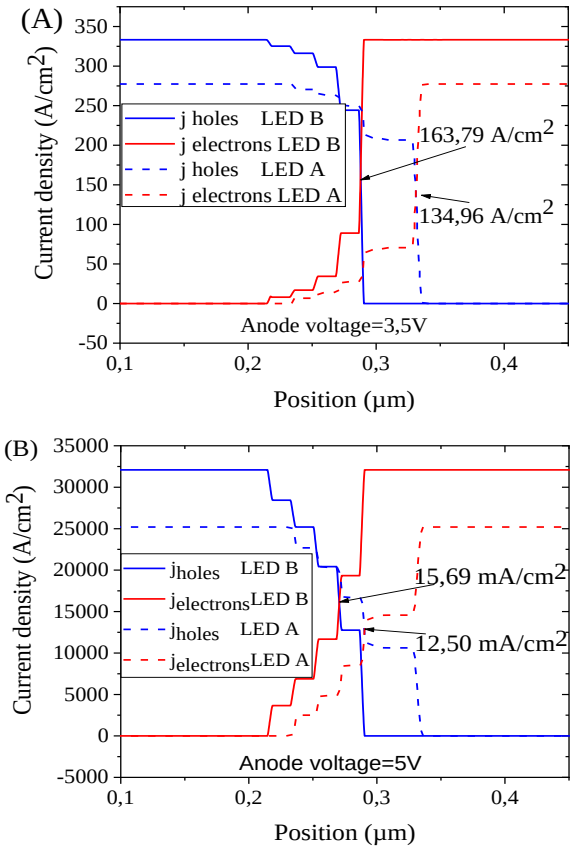

Figure 3. Distribution of electron and hole current density for the two LEDs

These findings demonstrate that including an n-type EBL considerably lowers electron leakage while simultaneously improving carrier confinement in the active region. In fact, compared to LED A, the value of electron leakage in LED B is much smaller, at 0.07A/cm². By encouraging improved electron-hole matching and lowering losses from non-radiative recombination, this decrease in leakage is essential for raising the LED's overall efficiency.

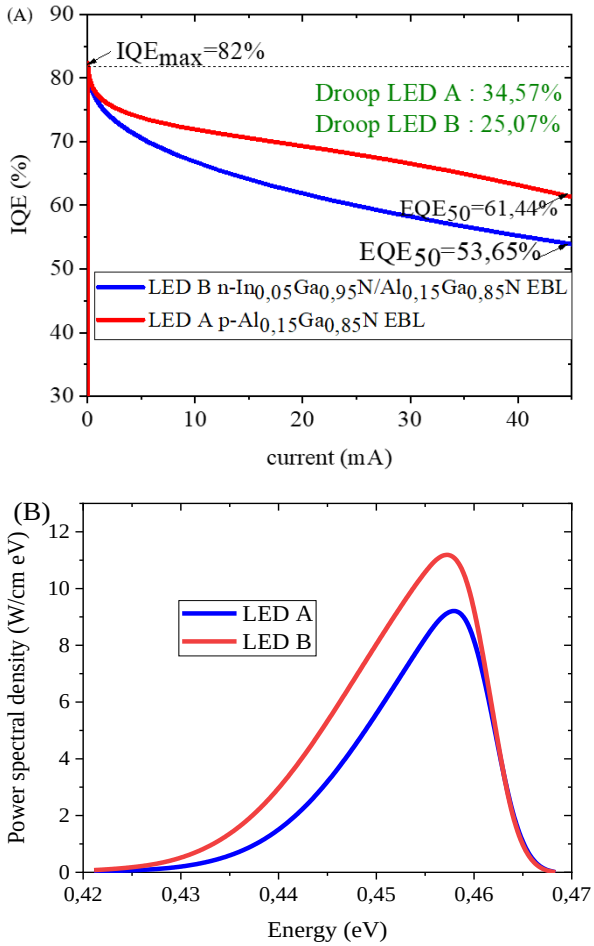

Figure 4. (A) Internal quantum efficiency; (B) power spectral density of LED A and LED B

Figure 4 (A) shows the internal quantum efficiency (IQE) of LEDs A and B as a function of injection current. With current, the IQE of both structures rises to a high of around 82% before beginning to fall. This decline, also referred to as "efficiency droop," is a well-known problem in InGaN-based LEDs and is frequently caused by Auger recombination, electron overflow, and an imbalance between electron and hole injection. Because carrier confinement is less successful in LED A, which employs a traditional p-$Al_{0.15}Ga_{0.85}N$ electron blocking layer (EBL), efficiency droop becomes more noticeable as current rises. In particular, LED B mitigates the IQE drop between 0 mA and 50 mA to 25.07% as opposed to 34.57% in LED A, decrease of approximately 9.5%. Additionally, the improvement in IQE from 53.65% to 61.44% at 50mA represents a gain of 7.79%. Better electron confinement afforded by the multi-layer n-type EBL structure composed of $In_{0.05}Ga_{0.95}N/Al_{0.15}Ga_{0.85}N$ is responsible for the improvement shown in LED B. This n-type EBL facilitates improved hole injection into the quantum wells while more successfully preventing electron overflow out of the active region. Better carrier dispersion lowers the possibility of non-radiative recombination, which is more common at higher injection currents in LED A and includes Shockley-Read-Hall (SRH) and Auger recombination. Additionally, the power spectral density of LEDs A and B at 5V bias is shown as a function of energy in Figure 4 (B). Both LEDs exhibit a single emission peak at a wavelength of around 460nm, which is indicative of blue emission. But compared to LED A, LED B has a larger power spectrum density, suggesting more effective

radiative recombination (the improved in the LED B shows a significant increase of 23.3%). This may be explained by the n-type EBL's enhanced carrier confinement and decreased electron overflow. In contrast to an LED with a high indium concentration, the EBL's incorporation of $In_{0.05}Ga_{0.95}N$ layers helps minimise electron overflow and enhances hole injection efficiency while keeping the indium concentration low, protecting the quality of the InGaN alloy and lowering the Stark effect.

Figure 5 illustrates a discernible rise in radiative recombination rates at 5V bias in all five quantum wells in LED A and LED B. This figure shows an increase in the radiative recombination rate in the LED B particularly at 0.288µm where the rate reaches $1.027.10^{29}$ $cm^{-3}s^{-1}$. The addition of an n-type $In_{0.05}Ga_{0.95}N/Al_{0.15}Ga_{0.85}N$ electron blocking layer (EBL) is directly responsible for this enhancement. This EBL has two functions: it decreases electron overflow and improves both electron and hole injection into the active region. However, since some electrons flow through the quantum wells without taking part in recombination, LED A, which uses a traditional p-type EBL, experiences electron leakage, which lowers efficiency. Improved charge carrier management is responsible for the significant improvement in LED B's performance. Because the traditional EBL is less successful at preventing extra electrons from entering the active region, electron leakage occurs in LED A. Additionally, LED A exhibits poorer hole injection, especially at the interface between the p-EBL and the quantum wells. The imbalance between electrons and holes causes additional non-radiative recombination pathways, such Shockley-Read-Hall recombination, which further inhibits radiative recombination. In contrast, the n-type EBL in LED B enables greater hole injection into the quantum wells in addition to improving electron confinement. The rates are greater across all quantum wells in LED B because of the more favourable conditions for radiative recombination created by this balanced injection of carriers. Additionally, this reduces non-radiative losses like Auger recombination, which usually cause efficiency to droop at larger injection currents.

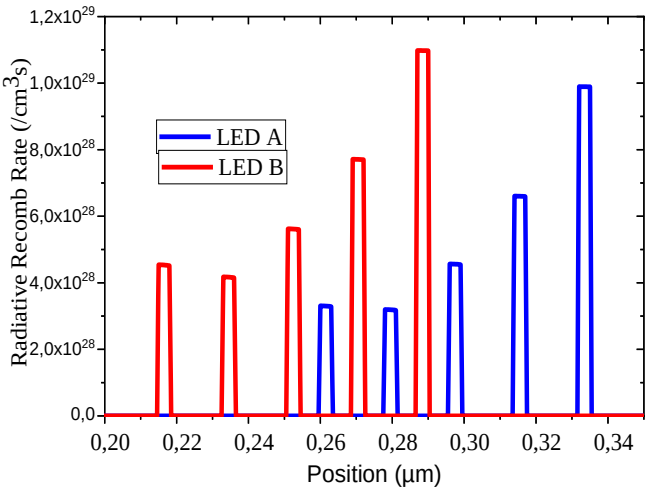

Figure 5. Radiative recombination rate in the active region of LED A and LED B at 5V bias

5. CONCLUSIONS

We investigated the impact of an n-type electron blocking layer (EBL) composed of $In_{0.05}Ga_{0.95}N/Al_{0.15}Ga_{0.85}N$ (Mg-doping=1×10^{19} cm^{-3}) placed between the active region and the n-GaN cladding layer in a light-emitting diode device functioning at about ~460nm. The performance characteristics of these structure is compared to the conventional p – type EBL. Based on modelling and simulation, the n-type $In_{0.05}Ga_{0.95}N/Al_{0.15}Ga_{0.85}N$ EBL may improve radiative recombination by reducing electron overflow and increasing hole injection efficiency into the active region of the structure. Additionally, when switching from the p-type $Al_{0.15}Ga_{0.85}N$ EBL to the n-type $In_{0.05}Ga_{0.95}N/Al_{0.15}Ga_{0.85}N$. The droop is improved from 34.57% to 25.07%. This indicates that the proposed structure LED B reduces efficiency losses at high injection. A 21.38% increase in current density at 3.5 V was observed, signifying more efficient carrier injection into the active region. the radiative recombination rate in the LED B achieved maximum values of 1.02×10^{29} $cm^{-3}\cdot s^{-1}$ at 0.28µm, affirming to a significant improvement of the radiative process. Finally, the progress of the IQE, going from 53.65% to 61.44% at 50mA, as well as the maximum IQE reaching 82%, show a good radiative recombination in the LED B. However, Introducing InGaN layers in n-type EBL seems to be an efficient solution to reduce electron overflow and enhance hole injection efficiency by keeping a low indium concentration. These results confirm that the structure LED offers a substantial improvement in the performance of GaN/InGaN-based LEDs, particularly for applications requiring increased efficiency at moderate to high injection currents.

REFERENCES

[1] Pandey, A., Shin, W.J., Liu, X., Mi, Z. (2019). Effect of electron blocking layer on the efficiency of AlGaN mid-ultraviolet light emitting diodes. Optics Express, 27(12): A738-A745. http://doi.org/10.1364/OE.27.00A738

[2] Park, J.H., Yeong Kim, D., Hwang, S., Meyaard, D., Fred Schubert, E., Dae Han, Y., Choi, J.W., Cho, J., Kyu Kim, J. (2013). Enhanced overall efficiency of GaInN-based light-emitting diodes with reduced efficiency droop by Al-composition-graded AlGaN/GaN superlattice electron blocking layer. Applied Physics Letters, 103(6): 061104. https://doi.org/10.1063/1.4817800

[3] Usman, M., Munsif, M., Anwar, A.R., Jamal, H., Malik, S., Islam, N.U. (2020). Quantum efficiency enhancement by employing specially designed AlGaN electron blocking layer. Superlattices and Microstructures, 139: 106417. https://doi.org/10.1016/j.spmi.2020.106417

[4] Usman, M., Anwar, A.R., Saba, K., Munsif, M. (2020). Thickness-graded quantum barriers and composition-graded electron blocking layer for efficient green light-emitting diodes. Optik, 215: 164767. https://doi.org/10.1016/j.ijleo.2020.164767

[5] Dai, Q., Zhang, X., Wu, Z., Zeng, X., Wang, S. (2022). High performance of a non-polar AlGaN-based DUV-LED with a quaternary superlattice electron blocking layer. Journal of Electronic Materials, 51(9): 5389-5394. https://doi.org/10.1007/s11664-022-09778-2

[6] Yadav, G., Dewan, S., Tomar, M. (2022). Electroluminescence study of InGaN/GaN QW based pin and inverted pin junction based short-wavelength LED device using laser MBE technique. Optical Materials, 126: 112149. https://doi.org/10.1016/j.optmat.2022.112149

[7] Ren, Z., Lu, Y., Yao, H.H., Sun, H., Liao, C.H., Dai, J., Chen, C., Ryou, J.H., Yan, J., Wang, J., Li, J., Li, X. (2019). III-nitride deep UV LED without electron blocking layer. IEEE Photonics Journal, 11(2): 1-11. https://doi.org/10.1109/jphot.2019.2902125

[8] Chen, Y., Wu, H., Han, E., Yue, G., Chen, Z., Wu, Z., Wang, G., Jiang, H. (2015). High hole concentration in p-type AlGaN by indium-surfactant-assisted Mg-delta doping. Applied Physics Letters, 106(16). https://doi.org/10.1063/1.4919005

[9] Liang, Y.H., Towe, E. (2018). Progress in efficient doping of high aluminum-containing group III-nitrides. Applied Physics Reviews, 5(1): 011107. https://doi.org/10.1063/1.5009349

[10] Li, L., Zhang, Y., Xu, S., Bi, W., Zhang, Z.H., Kuo, H.C. (2017). On the hole injection for III-nitride based deep ultraviolet light-emitting diodes. Materials, 10(10): 1221. https://doi.org/10.3390/ma10101221

[11] Zhang, Z.H., Huang Chen, S.W., Chu, C., Tian, K., Fang, M., Zhang, Y., Bi, W., Kuo, H.C. (2018). Nearly efficiency-droop-free AlGaN-based ultraviolet light-emitting diodes with a specifically designed superlattice p-type electron blocking layer for high Mg doping efficiency. Nanoscale Research Letters, 13: 1-7. https://doi.org/10.1186/s11671-018-2539-9

[12] Al Tahtamouni, T.M., Sedhain, A., Lin, J.Y., Jiang, H.X. (2008). Si-doped high Al-content AlGaN epilayers with improved quality and conductivity using indium as a surfactant. Applied Physics Letters, 92(9): 092105. https://doi.org/10.1063/1.2890416

[13] Taniyasu, Y., Kasu, M., Kobayashi, N. (2002). Intentional control of n-type conduction for Si-doped AlN and Al X Ga 1-XN (0.42≤x<1). Applied Physics Letters, 81(7): 1255-1257. https://doi.org/10.1063/1.1499738

[14] SILVACO International. (2006). ATLAS User's Manual, Device Simulation Software. http://ridl.cfd.rit.edu/products/manuals/Silvaco/atlas_users.pdf.

[15] Shockley, W.T.R.W., Read Jr, W.T. (1952). Statistics of the recombinations of holes and electrons. Physical Review, 87(5): 835. https://doi.org/10.1103/PhysRev.87.835

[16] Hall, R.N. (1952). Electron-hole recombination in germanium. Physical Review, 87(2): 387. https://doi.org/10.1103/PhysRev.87.387

[17] Auf der Maur, M., Galler, B., Pietzonka, I., Strassburg, M., Lugauer, H., Di Carlo, A. (2014). Trap-assisted tunneling in InGaN/GaN single-quantum-well light-emitting diodes. Applied Physics Letters, 105(13): 133504. https://doi.org/10.1063/1.4896970

[18] Piprek, J., Römer, F., Witzigmann, B. (2015). On the uncertainty of the Auger recombination coefficient extracted from InGaN/GaN light-emitting diode efficiency droop measurements. Applied Physics Letters, 106(10): 101101. https://doi.org/10.1063/1.4914833

[19] Zhao, H., Liu, G., Zhang, J., Arif, R.A., Tansu, N. (2013). Analysis of internal quantum efficiency and current injection efficiency in III-nitride light-emitting diodes. Journal of Display Technology, 9(4): 212-225. https://doi.org/10.1109/jdt.2013.2250252

[20] Schubert, M.F., Chhajed, S., Kim, J.K., Schubert, E.F., Koleske, D.D., Crawford, M.H., Lee; S.R., Fischer, A.J., Thaler, G., Banas, M.A. (2007). Effect of dislocation density on efficiency droop in GaInN⁄GaN light-emitting diodes. Applied Physics Letters, 91(23): 231114. https://doi.org/10.1063/1.2822442

[21] Shen, Y.C., Mueller, G.O., Watanabe, S., Gardner, N.F., Munkholm, A., Krames, M.R. (2007). Auger recombination in InGaN measured by photoluminescence. Applied Physics Letters, 91(14): 141101. https://doi.org/10.1063/1.2785135

[22] Son, J.K., Lee, S.N., Paek, H.S., Sakong, T., Ha, K.H., Nam, O.H., Park, Y. (2007). Radiative and non-radiative transitions in blue quantum wells embedded in AlInGaN-based laser diodes. Physica Status Solidi C, 4(7): 2780-2783. https://doi.org/10.1002/pssc.200674746

[23] Piprek, J. (2013). Semiconductor Optoelectronic Devices: Introduction to Physics and Simulation. Elsevier. Academic Press, UCSB. https://doi.org/10.1016/C2009-0-22633-X

[24] Ahmad, S., Raushan, M.A., Kumar, S., Dalela, S., Siddiqui, M.J., Alvi, P.A. (2018). Modeling and simulation of GaN based QW LED for UV emission. Optik, 158: 1334-1341. https://doi.org/10.1016/j.ijleo.2018.01.023

[25] Lu, S., Li, J., Huang, K., Liu, G., Zhou, Y., Cai, D., Zhang, R., Kang, J. (2021). Designs of InGaN micro-LED structure for improving quantum efficiency at low current density. Nanoscale Research Letters, 16(1): 99. https://doi.org/10.1186/s11671-021-03557-4

[26] Verzellesi, G., Saguatti, D., Meneghini, M., Bertazzi, F., Goano, M., Meneghesso, G., Zanoni, E. (2013). Efficiency droop in InGaN/GaN blue light-emitting diodes: Physical mechanisms and remedies. Journal of Applied Physics, 114(7): 071101. https://doi.org/10.1063/1.4816434

[27] Jamil, T., Usman, M., Malik, S., Jamal, H. (2021). The marvelous optical performance of AlGaN-based deep ultraviolet light-emitting diodes with AlInGaN-based last quantum barrier and step electron blocking layer. Applied Physics A, 127(5): 397. https://doi.org/10.1007/s00339-021-04559-w

[28] Hairol Aman, M.A., Ahmad Noorden, A.F., Abdul Kadir, M.Z., Danial, W.H., Daud, S. (2024). Effects of electron blocking layer thickness on the electrical and optical properties of AlGaN-Based deep-ultraviolet light-Emitting diode. Journal of Electronic Materials, 53: 4802-4811. https://doi.org/10.1007/s11664-024-11190-x

[29] Ahmad, S., Raushan, M.A., Gupta, H., Kattayat, S., Kumar, S., Dalela, S., Alvi, P.A., Siddiqui, M.J. (2019). Performance enhancement of UV quantum well light emitting diode through structure optimization. Optical and Quantum Electronics, 51: 243. https://doi.org/10.1007/s11082-019-1964-z

NOMENCLATURE

χ_e	electron affinity, eV
ε_r	permittivity
E_g	energy band gap, eV
m_n	electron effective mass
m_p	hole effective mass
C_{opt}	radiative recombination rate coefficient
Aug_n	electron Auger coefficient
Aug_p	hole Auger coefficient
τ_n	electron lifetime, s
τ_p	hole lifetime, s